The Canadian Mineralogist
Vol. 44, pp. 1197-1205 (2006)

REFINEMENT OF THE CRYSTAL STRUCTURE OF BILLIETITE, Ba $[(UO_2)_6\ O_4\ (OH)_6]\ (H_2O)_8$

ROBERT J. FINCH[§]

Department of Geological Sciences, University of Manitoba, Winnipeg, Manitoba R3T 2N2, Canada

PETER C. BURNS

Department of Civil Engineering and Geological Sciences, University of Notre Dame, Notre Dame, Indiana 46556, U.S.A.

FRANK C. HAWTHORNE[¶]

Department of Geological Sciences, University of Manitoba, Winnipeg, Manitoba R3T 2N2, Canada

RODNEY C. EWING

Department of Geology, University of Michigan, Ann Arbor, Michigan 48109, U.S.A.

ABSTRACT

The crystal structure of billietite, Ba $[(UO_2)_6\ O_4\ (OH)_6]\ (H_2O)_8$, orthorhombic, space group $Pbn2_1$, a 12.0941(8), b 30.211(2), c 7.1563(5) Å, V 2614.7(4) Å^3, Z = 4, has been refined to an R_1 index of 3.4% for 4918 unique observed ($|F_o| > 4\sigma F$) reflections measured with Mo$K\alpha$ X-radiation and a diffractometer fitted with a CCD detector. The structure consists of anionic $[(UO_2)_6\ O_4\ (OH)_6]^{2-}$ sheets, linked by interstitial Ba atoms and (H_2O) groups. There are two crystallographically distinct structural sheets and eight interlayer (H_2O) groups in billietite. Four (H_2O) groups are bonded to the interlayer Ba atoms, and the remaining four (H_2O) groups are not bonded to a cation, but are held in the structure by a network of hydrogen bonds.

Keywords: billietite, crystal structure, hydrogen bonding, uranyl oxide hydrate of Ba, uranium.

SOMMAIRE

Nous avons affiné la structure cristalline de la billietite, Ba $[(UO_2)_6\ O_4\ (OH)_6]\ (H_2O)_8$, orthorhombique, groupe spatial $Pbn2_1$, a 12.0941(8), b 30.211(2), c 7.1563(5) Å, V 2614.7(4) Å^3, Z = 4, jusqu'à un résidu R_1 de 3.4% en utilisant 4918 réflexions uniques observées ($|F_o| > 4\sigma F$) et mesurées avec rayonnement Mo$K\alpha$ et un diffractomètre muni d'un détecteur CCD. La structure est faite de feuillets anioniques $[(UO_2)_6\ O_4\ (OH)_6]^{2-}$ interconnectés par des atomes de Ba et des groupes H_2O interstitiels. Il y a deux sortes de feuillets, cristallographiquement distincts, et huit groupes H_2O interfoliaires. Quatre des groupes H_2O sont liés à des atomes de Ba entre les couches, et les quatre autres ne sont pas liés à un cation, mais font partie de la structure grâce à un réseau de liaisons hydrogène.

(Traduit par la Rédaction)

Mots-clés: billietite, structure cristalline, liaisons hydrogène, oxyde hydraté uranylé de Ba, uranium.

INTRODUCTION

Uranyl oxide hydrate minerals are common constituents of the oxidized parts of uranium deposits (Frondel 1958, Finch & Ewing 1992), as well as soils contaminated by actinides (Roh *et al*. 2000, Yamakawa & Traina 2001). Uranyl phases form by alteration of both UO_2 and spent nuclear fuel under conditions similar to those expected in the proposed geological repository at Yucca Mountain, Nevada (Finch & Ewing 1991, Forsyth & Werme 1992, Wronkiewicz *et al.* 1992, 1996, Johnson & Werme 1994, Finn *et al.* 1996). Studies of mineral

§ *Present address*: Argonne National Laboratory, 9700 South Cass Avenue, Argonne, Illinois 60439, U.S.A.
¶ *E-mail address*: frank_hawthorne@umanitoba.ca

occurrences can be used to test the extrapolation of results of short-term experiments to periods relevant to nuclear-waste disposal (Ewing 1993) and to assess models used to predict the long-term behavior of spent nuclear fuel in a geological repository (Bruno *et al.* 1995).

Billietite contains Ba, isotopes of which can occur as fission products in spent nuclear fuel. A phase with a structure similar to that of billietite, but that contains Cs, Ba, and Mo in addition to U, was reported in an investigation of oxidative corrosion of spent nuclear fuel in groundwater (Buck *et al.* 1998). Burns *et al.* (1997a) argued that uranyl phases, including uranyl oxide hydrates, that form owing to alteration of nuclear waste may incorporate various radionuclides in addition to uranium, thereby affecting radionuclide mobility. Uranyl oxide hydrates containing Sr and Cs have been documented (Hill & Burns 1999, Cahill & Burns 2000, Burns & Li 2002), and incorporation of trace levels of Np into the sodium analogue of the uranyl oxide hydrate compreignacite has recently been reported (Burns *et al.* 2004).

The crystal structures of most of the uranyl oxide hydrate minerals are now known: the structures of schoepite, metaschoepite, masuyite, protasite, becquerelite, compreignacite, curite, fourmarierite, wölsendorfite, vandendriesscheite, agrinierite and uranosphaerite have been reported (Hughes *et al.* 2003, and references therein). The structure of billietite was determined and refined to an agreement index (*R*) of 13.9% by Pagoaga *et al.* (1987) and is similar to the structures of becquerelite, protasite, compreignacite, masuyite, richetite, and agrinierite, each of which contain sheets of uranyl pentagonal bipyramids based upon the α-U_3O_8 anion topology (Burns 1999). Pagoaga *et al.* (1987) located only four (H_2O) groups *pfu* (per formula unit), rather than eight as indicated by previous and subsequent studies (Brasseur 1949, Frondel & Cuttita 1953, Christ & Clark 1960, Čejka *et al.* 1998). Because of the importance of (H_2O) to the structural stability and bonding in uranyl minerals (Finch *et al.* 1996, 1998, Finch 1997), we have redetermined the crystal structure of billietite in order to establish the role of the interlayer (H_2O) groups and to derive the scheme of interlayer hydrogen-bonding.

Experimental Methods

The specimen containing billietite was obtained from Mr. Forrest Cureton and is from Shaba, Democratic Republic of Congo. Several crystals were removed from the specimen and examined in cross-polarized light. Most crystals examined show signs of twinning; an untwinned crystal with sharp extinction and uniform optical properties was selected for study. The crystal was mounted on a Bruker Platform three-circle goniometer equipped with a 1K Smart CCD (charge-coupled device) detector and a crystal-to-detector distance of 5 cm.

The data were collected using monochromatic Mo*K*α X-radiation and frame widths of 0.3° in ω, with 20 s used to acquire each frame. A complete sphere of three-dimensional data was collected to ~57° 2θ. The final unit-cell dimensions (Table 1) were refined on the basis of 6558 reflections using least-squares techniques. Comparison of the intensities of equivalent reflections collected at different times during the data collection showed no evidence of significant change, and there was no streaking present in the diffraction pattern (*cf.* Pagoaga *et al.* 1987). The data were reduced and corrected for Lorentz, polarization and background effects using the Bruker program Saint. An empirical absorption-correction was done on the basis of 3724 intense reflections; the crystal was modeled as a {010} plate, and reflections with a plate-glancing angle of less than 3° were discarded from the dataset, which lowered *R*(azimuthal) from 31.8 to 6.2%. A total of 31,321 reflections was collected, of which 6814 were omitted because of a plate-glancing angle less than 3°. Merging of equivalent reflections gave 6104 unique reflections, with 4918 classed as observed ($|F_o| \geq 4\sigma_F$).

Structure Refinement

Scattering curves for neutral atoms, together with anomalous dispersion corrections, were taken from the *International Tables for X-Ray Crystallography, Vol. IV* (Wilson 1992). The Bruker Shelxtl Version 5 system of programs was used for refinement of the crystal structure.

Refinement of the structure was initiated in space group $Pbn2_1$ using the structure reported by Pagoaga *et al.* (1987) as the starting model. Following refinement of the positional parameters and isotropic-displacement parameters for all atoms, the agreement index R_1 was 6.3% for the observed reflections. Conversion of the cation-displacement parameters to an anisotropic form, together with refinement of the entire model, resulted in an R_1 index of 5.0%. Inspection of difference-Fourier maps at this stage revealed seven symmetrically distinct (H_2O) groups that were not present in the model of

TABLE 1. INFORMATION PERTAINING TO THE STRUCTURE REFINEMENT OF BILLIETITE

a (Å)	12.0941(8)	Crystal size (mm)	0.36 x 0.18 x 0.015
b (Å)	30.211(2)	Total reflections	24507
c (Å)	7.1563(5)	Unique reflections	6104
V (Å^3)	2614.7(4)	R_{int} (%)	6.2
Space group	$Pbn2_1$	Unique $\|F_o\| \geq 4\sigma_F$	4918
F(000)	3480	Final R_1 (%)	3.4
μ (mm^{-1})	38.62	*S*	1.03
D_{calc} (g/cm^3)	5.253	Flack parameter	0.06(1)

Unit-cell contents: Ba $[(UO_2)_6\ O_4\ (OH)_6]\ (H_2O)_8$

Pagoaga *et al.* (1987); insertion of the corresponding O-atoms into the model, together with full-matrix least-squares refinement of all variable parameters, resulted in a final R_1 index of 3.4% for the 4918 unique observed ($|F_o| \geq 4\sigma_F$) reflections, and a goodness-of-fit (S) of 1.03. A model including anisotropic displacement of the anions was tried, but it did not lower the final R_1 index, and refinement of site occupancies of the (H_2O) groups did not produce significant shifts from full occupancy. In the final cycle of refinement, the average parameter shift/esd was 0.000, and the maximum peaks in the final difference-Fourier maps were 1.6 and –2.8 e/Å^3. The final positional and anisotropic-displacement parameters are given in Tables 2 and 3, and selected interatomic distances and angles are given in Table 4. A bond-valence table, calculated with the universal U–O curve of Burns *et al.* (1997b) and the curves of Brown & Altermatt (1985) for Ba, is given in Table 5. Structure factors may be obtained from the Depository of Unpublished Data, CISTI, National Research Council of Canada, Ottawa, Ontario K1A 0S2, Canada.

Description of the Structure

Cation coordination

There are six symmetrically distinct *U* sites, all occupying general positions in space group $Pbn2_1$. Five of the six *U* sites are surrounded by seven anion sites in pentagonal–bipyramidal arrangements. Each of these $U\phi_7$ polyhedra [ϕ: (OH) and O] consists of two apical anions at distances of 1.78–1.83 Å from the central U atom, forming the $(U^{6+}O_2)^{2+}$ uranyl cation, and five equatorial anions [(OH) and O] at distances in the range 2.10–2.69 Å. The *U*(2) site is surrounded by six anion sites arranged at the vertices of a distorted octahedron. There are two uranyl O-atoms at distances

TABLE 2. COORDINATES AND EQUIVALENT ISOTROPIC-DISPLACEMENT PARAMETERS OF ATOMS IN THE STRUCTURE OF BILLIETITE

	x	*y*	*z*	U_{eq}
U(1)	0.55842(4)	0.74671(2)	0.00092(7)	0.0110(1)
U(2)	0.74723(3)	0.73833(2)	0.5391(1)	0.0116(1)
U(3)	0.93753(4)	0.74265(2)	0.99884(7)	0.0108(1)
U(4)	0.55865(4)	0.00466(2)	0.01958(6)	0.0113(1)
U(5)	0.94118(4)	0.00557(2)	0.01401(7)	0.0115(1)
U(6)	0.74929(3)	0.01411(2)	0.4481(1)	0.0113(1)
Ba	0.63786(6)	0.87627(2)	0.3155(2)	0.0206(2)
O(1)	0.5213(7)	0.6903(3)	0.952(1)	0.0200(19)
O(2)	0.5990(6)	0.8024(3)	0.058(1)	0.0176(18)
O(3)	0.7431(6)	0.6804(3)	0.599(1)	0.0183(19)
O(4)	0.7464(6)	0.7936(3)	0.445(1)	0.0171(17)
O(5)	0.9753(6)	0.6866(3)	0.952(1)	0.0169(18)
O(6)	0.8993(6)	0.7983(3)	0.052(1)	0.0202(19)
O(7)	0.6062(7)	0.9477(3)	0.032(1)	0.0232(19)
O(8)	0.5115(7)	0.0616(3)	0.011(1)	0.0166(17)
O(9)	0.8965(7)	0.9494(3)	0.980(1)	0.0230(22)
O(10)	0.9835(7)	0.0624(3)	0.039(1)	0.0190(19)
O(11)	0.7381(6)	0.9538(3)	0.473(1)	0.0194(22)
O(12)	0.7547(6)	0.0733(3)	0.432(1)	0.0116(16)
OH(13)	0.6016(6)	0.7238(2)	0.322(1)	0.0139(16)
O(14)	0.5935(7)	0.7558(3)	0.691(1)	0.0157(19)
O(15)	0.9038(7)	0.7496(3)	0.688(1)	0.0107(19)
OH(16)	0.8912(6)	0.7211(2)	0.322(1)	0.0139(16)
OH(17)	0.7464(6)	0.7244(3)	0.968(1)	0.0184(21)
O(18)	0.5779(6)	0.0136(2)	0.326(1)	0.0166(17)
OH(19)	0.6147(6)	0.0210(3)	0.697(1)	0.0137(18)
OH(20)	0.8880(6)	0.0229(3)	0.691(1)	0.0128(18)
O(21)	0.9161(6)	0.0043(3)	0.325(1)	0.0205(18)
OH(22)	0.7492(6)	0.0272(3)	0.076(1)	0.0152(18)
OW(23)	0.7739(7)	0.8733(4)	0.995(2)	0.0302(21)
OW(24)	0.9220(7)	0.6312(3)	0.314(2)	0.0319(22)
OW(25)	0.4129(8)	0.8883(3)	0.202(1)	0.0327(24)
OW(26)	0.9179(8)	0.1144(4)	0.690(1)	0.0382(26)
OW(27)	0.5645(8)	0.6345(3)	0.300(2)	0.0411(26)
OW(28)	0.7419(8)	0.6249(5)	0.025(2)	0.0539(34)
OW(29)	0.634(1)	0.8602(4)	0.696(1)	0.0523(30)
OW(30)	0.864(1)	0.8755(3)	0.390(1)	0.0452(32)

TABLE 3. ANISOTROPIC-DISPLACEMENT PARAMETERS FOR THE CATIONS IN THE STRUCTURE OF BILLIETITE

	U_{11}	U_{22}	U_{33}	U_{12}	U_{13}	U_{23}
U(1)	0.0093(2)	0.0153(2)	0.0084(3)	–0.0003(2)	–0.0001(2)	–0.0001(2)
U(2)	0.0079(2)	0.0154(3)	0.0115(2)	–0.0001(2)	–0.0005(2)	0.0006(2)
U(3)	0.0083(2)	0.0156(2)	0.0085(3)	0.0006(2)	–0.0001(2)	–0.0005(3)
U(4)	0.0091(2)	0.0172(2)	0.0076(2)	–0.0004(2)	–0.0005(2)	–0.0004(2)
U(5)	0.0093(2)	0.0173(2)	0.0079(2)	0.0003(2)	0.0004(2)	–0.0005(2)
U(6)	0.0067(2)	0.0166(3)	0.0104(2)	0.0002(2)	0.0000(2)	–0.0006(2)
Ba	0.0185(3)	0.0213(4)	0.0220(3)	–0.0011(3)	0.0003(4)	0.0005(3)

TABLE 4. SELECTED INTERATOMIC DISTANCES (Å) AND ANGLES (°) IN BILLIETITE

U(1)–O(1)a	1.795(9)	*U*(4)–O(8)	1.813(8)
U(1)–O(2)	1.799(8)	*U*(4)–O(7)e	1.816(9)
U(1)–O(14)a	2.276(8)	*U*(4)–O(18)	2.220(9)
U(1)–O(15)b	2.300(8)	*U*(4)–O(18)f	2.225(8)
U(1)–OH(17)a	2.382(8)	*U*(4)–OH(22)	2.437(7)
U(1)–OH(13)	2.46(1)	*U*(4)–OH(19)a	2.456(7)
U(1)–OH(16)b	2.583(8)	*U*(4)–OH(19)f	2.571(8)
<*U*(1)–O_{Ur}>	1.797	<*U*(4)–O_{Ur}>	1.814
<*U*(1)–φ_{eq}>	2.400	<*U*(4)–φ_{eq}>	2.382
U(2)–O(4)	1.802(9)	*U*(5)–O(9)g	1.798(9)
U(2)–O(3)	1.803(9)	*U*(5)–O(10)	1.799(9)
U(2)–O(15)	2.198(8)	*U*(5)–O(21)h	2.214(9)
U(2)–O(14)	2.217(8)	*U*(5)–O(21)	2.24(1)
U(2)–OH(13)	2.387(9)	*U*(5)–O(22)	2.451(7)
U(2)–OH(16)	2.391(8)	*U*(5)–O(20)a	2.455(7)
<*U*(2)–O_{Ur}>	1.802	*U*(5)–O(20)h	2.572(8)
<*U*(2)–φ_{eq}>	2.458	<*U*(5)–O_{Ur}>	1.798
		<*U*(5)–φ_{eq}>	2.386
U(2)–OH(17)	3.097(9)		
U(3)–O(6)c	1.783(8)	*U*(6)–O(12)	1.793(8)
U(3)–O(5)	1.786(8)	*U*(6)–O(11)e	1.83(1)
U(3)–O(15)	2.274(7)	*U*(6)–O(21)	2.222(8)
U(3)–O(14)d	2.335(8)	*U*(6)–O(18)	2.251(7)
U(3)–OH(17)	2.387(8)	*U*(6)–O(19)	2.422(7)
U(3)–OH(16)c	2.47(1)	*U*(6)–OH(20)	2.431(7)
U(3)–OH(13)d	2.561(8)	*U*(6)–O(22)	2.693(8)
<*U*(3)–O_{Ur}>	1.784	<*U*(6)–O_{Ur}>	1.811
<*U*(3)–φ_{eq}>	2.405	<*U*(6)–φ_{eq}>	2.404
Ba–*OW*(29)	2.77(1)	O(1)a–*U*(1)–O(2)	177.5(4)
Ba–*OW*(30)	2.79(1)	O(8)–*U*(4)–O(7)e	179.0(4)
Ba–*OW*(23)a	2.82(1)	O(4)–*U*(2)–O(3)	171.6(4)
Ba–*OW*(25)	2.86(1)	O(9)g–*U*(5)–O(10)	177.7(3)
Ba–O(11)	2.87(1)	O(6)c–*U*(3)–O(5)	178.6(4)
Ba–O(5)b	2.902(8)	O(12)–*U*(6)–O(11)e	177.1(3)
Ba–O(2)	2.931(8)		
Ba–O(8)i	2.957(8)		
Ba–O(4)	2.968(9)		
Ba–O(7)	2.986(8)		
<*Ba*–φ>	2.885		

a: $x, y, z-1$; b: $x-\frac{1}{2}, 1\frac{1}{2}-y, z-\frac{1}{2}$; c: $x, y, z+1$; d: $x+\frac{1}{2}, 1\frac{1}{2}-y, z+\frac{1}{2}$; e: $x, y-1, z$; f: $1-x, -y, z-\frac{1}{2}$; g: $x, y-1, z-1$; h: $2-x, -y, z-\frac{1}{2}$; i: $1-x, 1-y, z+\frac{1}{2}$.

of 1.80 Å and four meridional O and (OH) anions at distances in the range 2.20–2.39 Å. Calculation of the incident valence at the *U* sites using the coordination-independent parameters for the U–O bond (Burns *et al.* 1997b) indicates that U is in the hexavalent state at all sites (as indicated also by the presence of uranyl anions around all *U* sites). Calculation of the incident valence at the *U*(2) site using the parameters for the U_r –ϕ_4 ($^{[6]}$U–ϕ) bond (Burns *et al.* 1997b) gave an incident bond-valence of 5.97 *vu* (valence units), indicating that a coordination number of [6] is appropriate at the *U*(2) site. The structure of billietite shows distinct pseudo-symmetry in which the cations at the *U*(2) and *U*(6) sites are (pseudosymmetrically) related. Examination of Table 4 shows that the closest six *U*–ϕ distances involving each of these sites are similar, but the seventh-longest distances are very different: *U*(2)–OH(17) = 3.097(9) Å, whereas *U*(6)–O(22) = 2.693(8) Å.

TABLE 5. BOND-VALENCE ANALYSIS* FOR THE STRUCTURE OF BILLIETITE

	U(1)	*U*(2)	*U*(3)	*U*(4)	*U*(5)	*U*(6)	*Ba*	Σ
O(1)	1.63							1.63
O(2)	1.62						0.18	1.80
O(3)		1.63						1.63
O(4)		1.63					0.16	1.78
O(5)			1.66				0.19	1.85
O(6)			1.67					1.67
O(7)				1.57			0.15	1.72
O(8)				1.58			0.16	1.74
O(9)					1.62			1.62
O(10)					1.62			1.62
O(11)						1.52	0.21	1.73
O(12)						1.64		1.64
OH(13)	0.44	0.57	0.37					1.38
O(14)	0.64	0.77	0.57					1.98
O(15)	0.61	0.8	0.64					2.05
OH(16)	0.35	0.56	0.44					1.35
OH(17)	0.52		0.51					1.03
O(18)				0.71		0.67		2.08
				0.70				
OH(19)				0.45		0.48		1.29
				0.36				
OH(20)					0.45	0.47		1.28
					0.36			
O(21)					0.72	0.71		2.11
					0.68			
OH(22)				0.46	0.45	0.28		1.19
OW(23)							0.24	0.24
OW(24)								0
OW(25)							0.21	0.21
OW(26)								0
OW(27)								0
OW(28)								0
OW(29)							0.28	0.28
OW(30)							0.26	0.26
Σ	5.80	5.96	5.85	5.82	5.89	5.76	2.04	

* calculated using the parameters of Brown & Altermatt (1985) for Ba^{2+} and of Burns *et al.* (1997b) for U^{6+}, and given in *vu* (valence units).

The Ba atom is coordinated by six uranyl-O atoms at distances from 2.77 to 2.99 Å, and four (H_2O) groups at distances from 2.77 to 2.86 Å. The Ba coordination (Table 4) is similar to that in protasite (Pagoaga *et al.* 1987) and guilleminite (Cooper & Hawthorne 1995).

Bond topology

There are two symmetrically and stereochemically distinct sheets of uranyl polyhedra in the crystal structure of billietite (Fig. 1). The first sheet (Fig. 1a) consists of three uranyl polyhedra, *U*(1), *U*(2) and *U*(3), that share edges and corners to form a sheet identical to that in ianthinite (Burns *et al.* 1997c) and wyartite (Burns & Finch 1999). Chains of edge-sharing *U*(1) and *U*(3) pentagonal bipyramids extend in the *c* direction and are linked by sharing corners and by sharing edges with *U*(2) octahedra. In terms of the chain types used by Miller *et al.* (1996) to describe sheet-anion patterns, this arrangement forms a PU'PU'...sequence, where U'

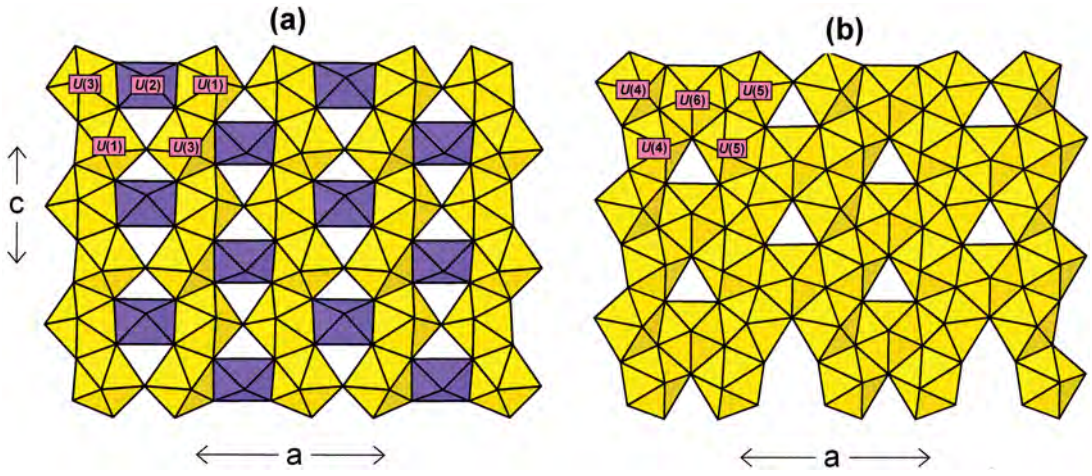

FIG. 1. The structural sheets of uranyl polyhedra in billietite projected along the *b* axis; (a) sheet of *U*(1), *U*(2) and *U*(3) polyhedra; (b) sheet of *U*(4), *U*(5), and *U*(6) polyhedra; *U*(2): mauve; other *U* polyhedra: yellow.

denotes a modification of the U chain type (Miller *et al.* 1996). The second sheet (Fig. 1b) also consists of three uranyl polyhedra, *U*(4), *U*(5) and *U*(6), that share edges and corners to form a sheet identical to that in protasite, becquerelite and compreignacite (Burns 1998). Separate chains of edge-sharing *U*(4) pentagonal bipyramids and *U*(6) pentagonal bipyramids extend in the *c* direction and are linked by sharing corners with each other and through the sharing of edges with *U*(6) pentagonal bipyramids, forming a PUPU... sequence (Miller *et al.* 1996). The (OH) groups in the second sheet (Fig. 1b) occur at the vertices of the unoccupied triangles, and the (OH) groups in the first sheet (Fig. 1a) occur at the vertices of the unoccupied triangle pointing downward in the figure. Thus the distribution of the (OH) groups in each sheet is the same, although the coordination number of OH(17) is one less than the coordination number of the pseudosymmetrically related OH(22) owing to the coordination difference between *U*(2) and *U*(6) (Table 5).

These sheets alternate along the *b* direction (Fig. 2) and are linked by interstitial [10]-coordinated Ba atoms and hydrogen bonding involving interstitial (H_2O) groups. The linkage between sheets is shown in more detail in Figure 3. There is a pseudo-mirror plane orthogonal to *b* whereby *U*(1) is related to *U*(4), *U*(2) to *U*(6), and *U*(3) to *U*(5). As indicated above, the principal difference between the two sheets involves the difference in coordination of *U*(2) and *U*(6), but inspection of Figure 3 shows that, in addition to this difference in coordination, there are significant geometrical differences in the tilting of the polyhedra in each sheet.

Interlayer (*H_2O*) *groups*

There are eight O-atom sites in the interlayer of billietite, and bond-valence calculations indicate that they are all are (H_2O) groups (Table 5). The OW(23), OW(25), OW(29) and OW(30) groups are bonded to Ba, whereas OW(24), OW(26), OW(27) and OW(28) are not. The arrangement of the (H_2O) groups in billietite is similar to the interlayer configuration in becquerelite (Burns & Li 2002).

Hydrogen Bonding in Billietite

Hydrogen-bonding plays a key role in the structural connectivities and stabilities of hydrated minerals (Hawthorne 1992), and nearly all minerals containing the uranyl ion also contain essential (H_2O) groups (Burns *et al.* 1996, Finch 1997). Because H atoms can rarely be located in difference-Fourier maps for highly absorbing materials, the accurate determination of *U*–O bond lengths (especially those for the uranyl ion) provides the best information for deriving hydrogen-bond interactions between the structural unit and interstitial (interlayer) (H_2O) groups in U minerals (Finch *et al.* 1996), although the difference in X-ray scattering for U and O can make accurate determination of the short uranyl (U–O) bond-length difficult (Finch *et al.* 1999).

Hydroxyl groups

There are six symmetrically distinct (OH) groups in the structural unit of billietite, and inspection of the bond-valence table (Table 5) indicates that each must act as a bond-valence donor to one or more interstitial (H_2O) groups. In most cases, inspection of the (OH)–OW distances unambiguously indicates the acceptor (H_2O) groups (Table 6). Note that OW(28) is an acceptor for hydrogen bonds from both OH(17) and OH(22), and that the corresponding OH–OW distances are significantly longer (~3.00 Å) than for those (H_2O) groups that accept just one hydrogen bond from the (OH) groups (~2.75 Å).

(*H_2O*) *groups: general considerations*

There are eight symmetrically distinct (H_2O) groups in the interlayer region of billietite. As noted above, five of these groups act as bond-valence acceptors for hydrogen bonds from (OH) groups of the uranyl sheet. The remaining (H_2O) groups [OW(23), OW(25), OW(29) and OW(30)] bond to the interstitial Ba atom. Note that OW(25) bonds to Ba *and* is a hydrogen-bond acceptor, and is the only (H_2O) group in billietite to exhibit this coordination.

(*H_2O*)...*O hydrogen bonding*

Inspection of the bond-valence table for billietite (Table 5) shows that there are twelve O atoms [O(1) to O(12)] that receive significantly less than 2.0 *vu* from their coordinating U and Ba atoms, and hence must be hydrogen-bond acceptors. Thus *at least* twelve donor bonds involving interstitial (H_2O) groups must also involve O atoms of the uranyl sheet; these interactions may be identified from the observed OW–O distances. The O(6), O(9) and O(11) atoms each have only one (H_2O) group within range of strong to medium hydrogen-bonding: OW(23), OW(23) and OW(30), respectively (Table 6). As OW(23) is involved in two medium-strength hydrogen bonds, with O(6) and O(9), O(2) and O(7) must accept hydrogen bonds from OW(29) and OW(25), as these are the only other (H_2O) groups within range. The O(1)–OW(30) distance is 2.79 Å, whereas the other O(1)–OW distances are greater than 3.0 Å; as the O(1) anion shows a considerable bond-valence deficiency, if one considers only its coordinating U atoms, a strong hydrogen-bonding interaction is required, and hence we assign this interaction to O(1)–OW(30) (Table 6). As OW(30) is now involved in two hydrogen bonds, O(4) must be an acceptor anion for OW(29) (Table 6). This leaves O(5) and O(8), with distances to OW(24) and OW(25) between 2.83 and

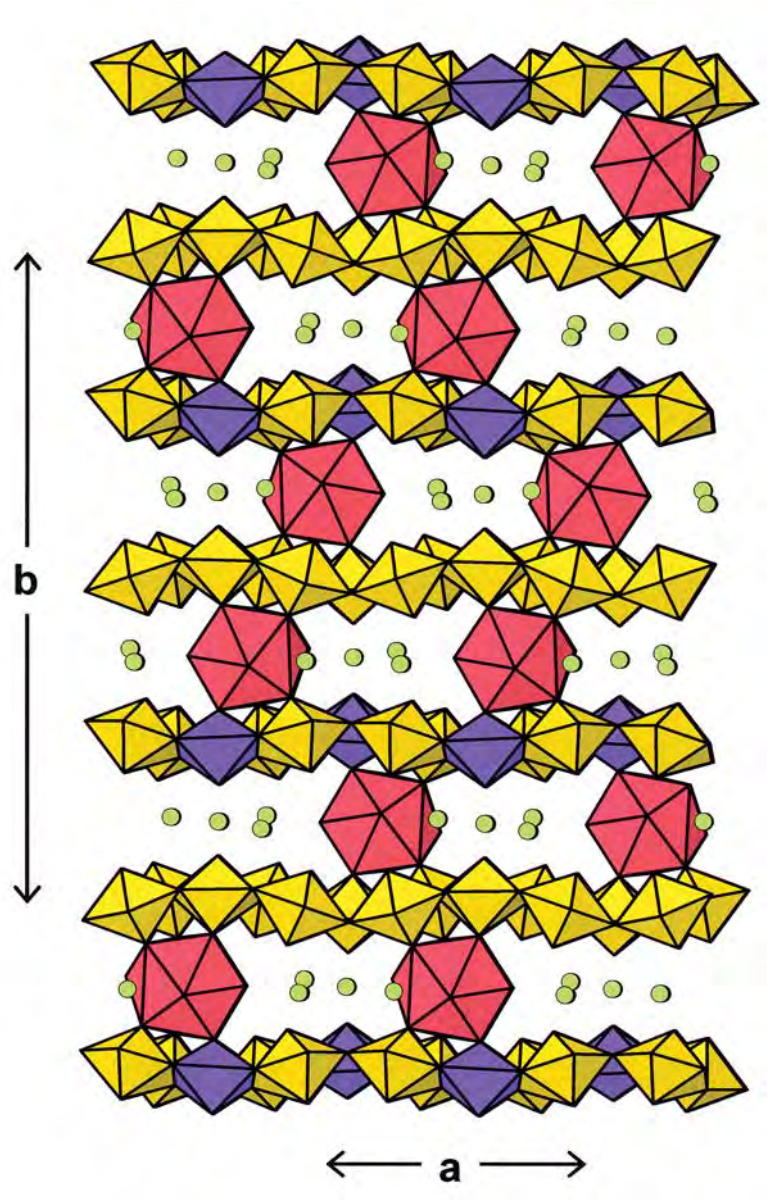

FIG. 2. The crystal structure of billietite projected down the *c* axis. Legend as in Figure 1; the Ba polyhedra are shown in red, and the interstitial (H_2O) groups are shown as green circles.

3.15 Å; considering the bond-valences incident at O(5) (1.85 *vu*) and O(8) (1.74 *vu*) from their coordinating U and Ba atoms, the O(8)–OW interaction was assigned to the shorter distance [O(8)–OW(25) 2.83 Å]. The latter assignment forces O(3) to be an acceptor for OW(26). The O(10) and O(12) are assigned as acceptors to the closest remaining (H_2O) groups OW(27) and OW(24), respectively. All assignments are listed in Table 6.

(*H_2O*)...(*H_2O*) *hydrogen bonding*

All (H_2O) groups involved only in hydrogen bonds were assumed to be [4]-coordinated (by H atoms). This

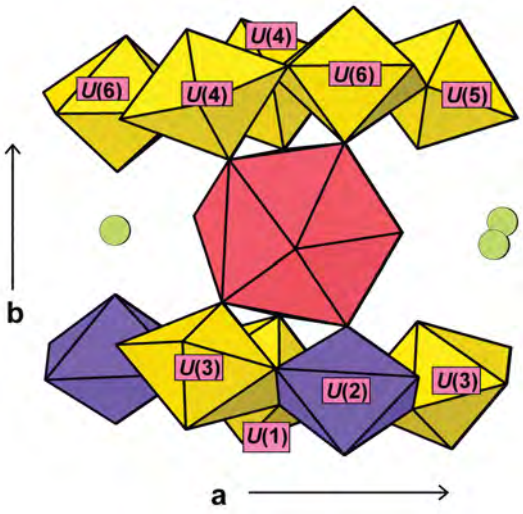

FIG. 3. Details of the linkage of polyhedra around the *Ba* site in billietite; legend as in Figure 2.

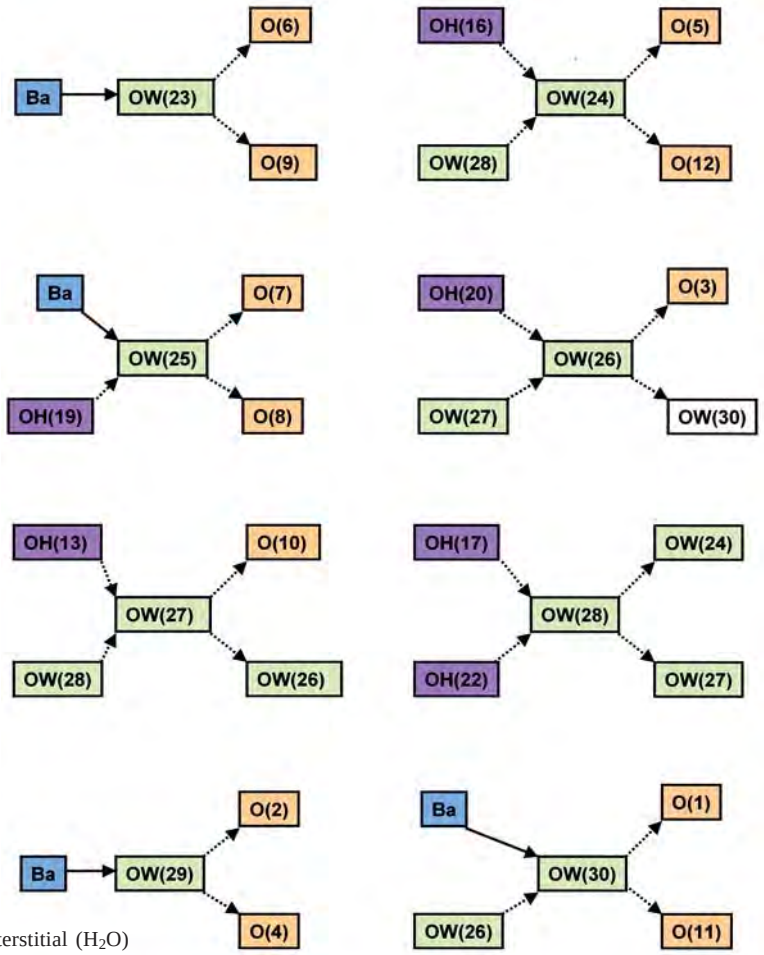

FIG. 4. The bonds around each interstitial (H_2O) group in billietite.

being the case, only one arrangement of hydrogen bonds is possible; the relevant interatomic distances are given in Table 6. The arrangement of bonds around each (H_2O) group in billietite is shown in Figure 4.

Acknowledgements

We thank Mr. Forrest Cureton for the crystal used in this study, Thomas Albrecht-Schmidt, J. Sejkora and Associate Editors Uwe Kolitsch and Sergey V. Krivovichev for their comments on the manuscript, and the distant pen of Bob Martin for his inimitable clarifications. This research was funded by the Environmental Management Sciences Program of the United States Department of Energy (DE–FG07–97ER14820) grant to PCB, and the Natural Sciences and Engineering Research Council of Canada grants to FCH and a International Postdoctoral Fellowship to RJF.

References

Brasseur, H. (1949): Étude de la billietite. *Bull. Acad. Roy. Belg., Cl. Sci.* **35**, 793-804.

Brown, I.D. & Altermatt, D. (1985): Bond-valence parameters obtained from a systematic analysis of the inorganic crystal structure database. *Acta Crystallogr.* **B41**, 244-247.

Bruno, J., Casas, I., Cera, E., Ewing, R.C., Finch, R.J. & Werme, L.O. (1995): The assessment of the long-term evolution of the spent nuclear fuel matrix by kinetic, thermodynamic and spectroscopic studies of uranium minerals. *Mater. Res. Soc., Symp. Proc.* **353**, 633-639.

Buck, E.C., Finch, R.J., Finn, P.A. & Bates, J.K. (1998): Retention of neptunium in uranyl alteration phases formed during spent fuel corrosion. *Mater. Res. Soc., Symp. Proc.* **506**, 83-91.

Burns, P.C. (1998): The structure of compreignacite, $K_2[(UO_2)_3O_2(OH)_3]_2(H_2O)_7$. *Can. Mineral.* **36**, 1061-1067.

Burns, P.C. (1999): The crystal chemistry of uranium. *In* Uranium: Mineralogy, Geochemistry and the Environment (P.C. Burns & R. Finch, eds.). *Rev. Mineral.* **38**, 23-90.

Burns, P.C., Deely, K.M. & Skanthakumar, S. (2004): Neptunium incorporation into uranyl compounds that form as alteration products of spent nuclear fuel: implications for geologic repository performance. *Radiochim. Acta* **92**, 151-159.

Burns, P.C., Ewing, R.C. & Hawthorne, F.C. (1997b): The crystal chemistry of hexavalent uranium: polyhedron geometries, bond valence parameters, and polymerization of polyhedra. *Can. Mineral.* **35**, 1551-1570.

Burns, P.C., Ewing, R.C. & Miller, M.L. (1997a): Incorporation mechanisms of actinide elements into the structures of U^{6+} phases formed during the oxidation of spent nuclear fuel. *J. Nucl. Mater.* **245**, 1-9.

Burns, P.C. & Finch, R.J. (1999): Wyartite: crystallographic evidence for the first pentavalent-uranium mineral. *Am. Mineral.* **84**, 1456-1460.

Burns, P.C., Finch, R.J., Hawthorne, F.C., Miller, M.L. & Ewing, R.C. (1997c): The crystal structure of ianthinite, $[U^{4+}{}_2(UO_2)_4O_6(OH)_4(H_2O)_4](H_2O)_5$: a possible phase for Pu^{4+} incorporation during the oxidation of spent nuclear fuel. *J. Nucl. Mater.* **249**, 199-206.

Burns, P.C. & Li, Yaping (2002): The structures of becquerelite and Sr-exchanged becquerelite. *Am. Mineral.* **87**, 550-557.

Burns, P.C., Miller, M.L. & Ewing, R.C. (1996): U^{6+} minerals and inorganic phases: a comparison and hierarchy of crystal structures. *Can. Mineral.* **34**, 845-880.

Cahill, C.L. & Burns, P.C. (2000): The structure of agrinierite: a Sr-containing uranyl oxide hydrate mineral. *Am. Mineral.* **85**, 1294-1297.

Christ, C.L. & Clark, J.R. (1960): Crystal chemical studies of some uranyl oxide hydrates. *Am. Mineral.* **45**, 1026-1061.

Cooper, M.A. & Hawthorne, F.C. (1995): The crystal structure of guilleminite, a hydrated Ba–U–Se sheet structure. *Can. Mineral.* **33**, 1103-1109.

Čejka, J., Sejkora, J., Skála, R., Čejka, J., Novotná, M. & Ederová, J. (1998): Contribution to the crystal chemistry of synthetic becquerelite, billietite and protasite. *Neues Jahrb. Mineral., Abh.* **174**, 159-180.

Ewing, R.C. (1993): The long-term performance of nuclear waste forms: natural materials – three case studies. *Mater. Res. Soc., Symp. Proc.* **294**, 559-568.

Finch, R.J. (1997): The role of H_2O in minerals containing the uranyl ion. *Am. Geophys. Union, Trans.* (*Eos*) **78**, S328 (abstr.).

Finch, R.J., Cooper, M.A., Hawthorne, F.C. & Ewing, R.C. (1996): The crystal structure of schoepite, $[(UO_2)_8O_2(OH)_{12}](H_2O)_{12}$. *Can. Mineral.* **34**, 1071-1088.

Finch, R.J., Cooper, M.A., Hawthorne, F.C. & Ewing, R.C. (1999): Refinement of the crystal structure of rutherfordine. *Can. Mineral.* **37**, 929-938.

Finch, R.J. & Ewing, R.C. (1991): Uraninite alteration in an oxidizing environment and its relevance to the disposal of spent nuclear fuel. *SKB Tech. Rep.* **91-15**.

Finch, R.J. & Ewing, R.C. (1992): The corrosion of uraninite under oxidizing conditions. *J. Nucl. Mater.* **190**, 133-156.

Finch, R.J., Hawthorne, F.C. & Ewing, R.C. (1998): Structural relations among schoepite, metaschoepite and "dehydrated schoepite." *Can. Mineral.* **36**, 831-846.

FINN, P.A., HOH, J.C., WOLF, S.F., SLATER, S.A. & BATES, J.K. (1996): The release of uranium, plutonium, cesium, strontium, technetium and iodine from spent fuel under unsaturated conditions. *Radiochim. Acta* **74**, 65-71.

FORSYTH, R.S. & WERME, L.O. (1992): Spent fuel corrosion and dissolution. *J. Nucl. Mater.* **190**, 3-19.

FRONDEL, C. (1958): Systematic mineralogy of uranium and thorium. *U.S. Geol. Surv., Bull.* **1064**.

FRONDEL, C. & CUTTITA, F. (1953): Studies of uranium minerals. XII. The status of billietite and becquerelite. *Am. Mineral.* **38**, 1019-1024.

HAWTHORNE, F.C. (1992): The role of OH and H_2O in oxide and oxysalt minerals. *Z. Kristallogr.* **201**, 183-206.

HILL, F.C. & BURNS, P.C. (1999): Structure of a synthetic Cs uranyl oxide hydrate and its relationship to compreignacite. *Can. Mineral*. **37**, 1283-1288.

HUGHES, K.-A., BURNS, P.C. & KOLITSCH, U. (2003): The crystal structure and crystal chemistry of uranosphaerite, $Bi(UO_2)O_2OH$. *Can. Mineral.* **41**, 677-685.

JOHNSON, L.H. & WERME, L.O. (1994): Materials characteristic and dissolution behavior of spent nuclear fuel. *Mater. Res. Soc. Bull.* **19**(12), 24-27.

MILLER, M.L., FINCH, R.J., BURNS, P.C. & EWING, R.C. (1996): Description and classification of uranium oxide hydrate sheet topologies. *J. Mater. Res.* **11**, 3048-3056.

PAGOAGA, M.K., APPLEMAN, D.E. & STEWART, J.M. (1987): Crystal structures and crystal chemistry of the uranyl oxide hydrates becquerelite, billietite, and protasite. *Am. Mineral.* **72**, 1230-1238.

ROH, Y., LEE, S.R., CHOI, S.K., ELLES, M.P. & LEE, S.Y. (2000): Physiochemical and mineralogical characterization of uranium-contaminated soils. *Soil Sed. Contam.* **9**, 463-486.

WILSON, A.J.C., ed. (1992): *International Tables for X-ray Crystallography, Vol. C.* Kluwer Academic Press, Boston, Massachusetts.

WRONKIEWICZ, D.J., BATES, J.K., GERDING, T.J., VELECKIS, E. & TANI, B.S. (1992): Uranium release and secondary phase formation during unsaturated testing of UO_2 at 90°C. *J. Nucl. Mater.* **190**, 107-127.

WRONKIEWICZ, D.J., BATES, J.K., WOLF, S.F. & BUCK, E.C. (1996): Ten-year results from unsaturated drip tests with UO_2 at 90°C: implications for the corrosion of spent nuclear fuel. *J. Nucl. Mater.* **238**, 78-95.

YAMAKAWA, I. & TRAINA, S.J. (2001): Precipitation processes of uranium in highly alkaline solutions: possible chemical reactions occurring in the Hanford vadose zone. *Am. Chem. Soc., 222nd Nat. Meeting* (*Chicago*), *Abstr.* **GEOC-055**.

Received July 8, 2005, revised manuscript accepted June 1, 2006.

The Canadian Mineralogist
Vol. 44, pp. 1565-1566 (2006)

ERRATA

In the article on the crystal structure of (Be,□) $(V,Ti)_3O_6$, a mineral related to kyzylkumite, by Gunnar Raade and Tonči Balić-Žunić (*Can. Mineral.* **44**, 1147-1158), Figure 6 (page 1157) was submitted for printing in color. Owing to an error in the printing establishment, the figure was not printed in color, although it appears in color in the electronic copy. The figure is reprinted here correctly.

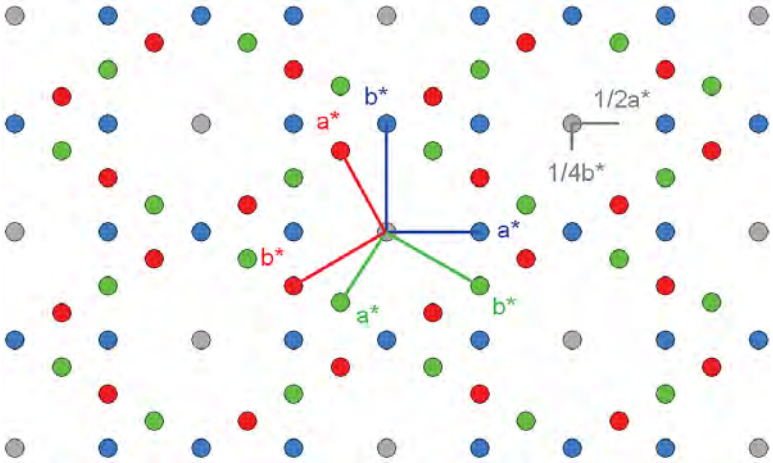

In the article on the refinement of the crystal structure of billietite, Ba $[(UO_2)_6\ O_4\ (OH)_6]\ (H_2O)_8$, by Robert J. Finch, Peter C. Burns, Frank C. Hawthorne and Rodney C. Ewing (*Can. Mineral.* **44**, 1197-1205), Table 6 was inadvertently left out by the typographer. The figure is reprinted here.

TABLE 6. CATION–ANION AND ANION–ANION CONTACTS (Å)* INVOLVING (H_2O) GROUPS AND HYDROGEN BONDS

OW(23)–Ba	2.82	OW(27)–OH(13)	2.74
OW(23)–O(6)	2.76	OW(27)–OW(28)	2.93
OW(23)–O(9)	2.74	OW(27)–O(10)	2.93
		OW(27)–OW(26)	2.86
OW(24)–OH(16)	2.74		
OW(24)–OW(28)	3.01	OW(28)–OH(17)	3.03
OW(24)–O(5)	3.15	OW(28)–OH(22)	2.98
OW(24)–O(12)	2.89	OW(28)–OW(24)	3.01
		OW(28)–OW(27)	2.93
OW(25)–Ba	2.86		
OW(25)–OH(19)	2.76	OW(29)–Ba	2.79
OW(25)–O(7)	3.19	OW(29)–O(2)	3.02
OW(25)–O(8)	2.83	OW(29)–O(4)	3.02
OW(26)–OH(20)	2.79	OW(30)–Ba	2.79
OW(26)–OW(27)	2.86	OW(30)–OW(26)	3.02
OW(26)–O(3)	2.86	OW(30)–O(1)	2.79
OW(26)–OW(30)	3.02	OW(30)–O(11)	2.88

* standard deviations 0.01–0.02 Å.

In the article on phase-equilibrium constraints on kiln temperatures at the Eby Pottery (*ca*. 1857–1905), Conestogo, Ontario, by J. Victor Owen and Jaroslav Dostal (*Can. Mineral.* **44**, 1257-1266), Table 1 was inadvertently left out by the typographer. The figure is reprinted here.

TABLE 1. BULK MAJOR-ELEMENT COMPOSITION OF EBY POTTERY

	Distorted samples			Undistorted samples		
	Eby1	Eby2	Eby3	Eby4	Eby5	Eby6
SiO_2 wt.%	69.4	66.4	68.2	68.7	65.8	69.5
TiO_2	0.8	0.9	0.8	0.8	0.7	0.6
Al_2O_3	14.4	15.0	14.3	14.3	14.1	13.6
FeO_T	3.8	5.8	5.7	4.9	5.0	4.3
MnO	0.1	0.1	0.1	0.1	0.2	0.1
MgO	2.1	2.2	2.1	2.2	2.4	2.3
CaO	3.4	3.4	2.0	3.5	6	3.6
Na_2O	2.2	1.5	1.9	1.7	1.8	1.9
K_2O	3.3	3.6	3.3	3.1	3.2	3.1
P_2O_5	0.4	1.1	1.6	0.7	0.8	0.9
Total	99.9	100.0	100.0	100.0	100.0	99.9

Data have been normalized to 100%. FeO_T: total Fe expressed as FeO.

Our apologies to the authors and readers for these errors.